13th Australasian Fluid Mechanics Conference
Monash University, Melbourne, Australia
13-18 December 1998

EULERIAN AND LAGRANGIAN STATISTICS OF PRESSURE GRADIENT FLUCTUATIONS IN ISOTROPIC TURBULENCE

Prakash VEDULA and P.K. YEUNG

School of Aerospace Engineering, Georgia Institute of Technology
Atlanta, GA 30332, USA

ABSTRACT

The statistics of pressure gradient fluctuations are studied in both Eulerian and Lagrangian frames of reference, using data from direct numerical simulations of isotropic turbulence. Relationships between pressure gradient fluctuations and the kinematics arising from vorticity and strain rate fluctuations are examined via one-point probability distributions. Lagrangian autocorrelations and frequency spectra of the pressure gradient and viscous contributions to the acceleration are computed directly for comparisons.

INTRODUCTION

The important role of pressure fluctuations in turbulence structure has been well recognized since Batchelor (1951). Much of the recent work (e.g., Hill & Wilczak 1995, Nelkin & Chen 1998) has focused on Eulerian properties such as one-point probability distributions and two-point correlations (and structure functions) in space, as well as possible connections to spatial flow structure such as intermittent regions of high vorticity (Pumir 1994). On the other hand, the Lagrangian properties of pressure gradient fluctuations are also important because they contribute dominantly to the fluid particle acceleration. In particular, particle-pair dispersion in turbulence is sensitive to the spatial structure of the flow via different types of local deformation. This provides our motivation to study the connection between pressure gradient and the vorticity and strain rate.

Our objective in this paper is to contribute to a more complete understanding of pressure gradient fluctuations in both Eulerian and Lagrangian frames of reference, using new data from direct numerical simulations (DNS). The simulation database is the same as that in a recent manuscript (Vedula & Yeung 1998), spanning a range of grid resolutions and Reynolds numbers as listed in Table 1. Here we consider primarily the probability density functions (PDFs) of the pressure gradient magnitude and its relationship to vorticity and strain rate fluctuations, as well as Lagrangian autocorrelations and frequency spectra. We first recall some definitions and describe briefly the method used to obtain Lagrangian pressure gradient fluctuations.

BACKGROUND AND METHOD

In usual notation, the acceleration vector in incompressible flow is given by

$$\underline{a} = -\nabla(p/\rho) + \nu\nabla^2\underline{u}\,. \qquad (1)$$

Pressure gradient fluctuations are known to have a variance much larger than that of the viscous acceleration (and increasingly so at high Reynolds numbers). They are also highly intermittent, with wide tails in the PDF. To explore connections with flow structure in isotropic turbulence, we consider here coordinate-frame invariant quantities, namely the magnitudes $|\nabla p|$ and $|\underline{\omega}|$ of pressure gradient and vorticity, and the effective strain rate $S \equiv (s_{ij}s_{ij})^{1/2}$. We note that for homogeneous turbulence $\langle\omega_i\omega_i\rangle = 2\langle S^2\rangle$.

According to recent Lagrangian results in DNS (Yeung 1997), the single-particle autocorrelation of acceleration decreases rapidly with time lag, and is characterized by a zero-crossing at about 2.2 Kolmogorov time scales (τ_η). It is of interest to study the corresponding autocorrelations of the pressure gradient and viscous contributions to the acceleration. Despite recent successes in Lagrangian measurements (Voth *etal* 1998) it is still very difficult to decompose the fluid particle acceleration unambiguously into its constituent terms (Eq. 1) in experiments. This task can, however, be accomplished using DNS as explained below.

We use the particle-tracking algorithm of Yeung & Pope (1988), in which Lagrangian variables are calculated from Eulerian fields by a cubic-spline interpolation scheme which is fourth-order accurate and twice continuously differentiable. This interpolation is applied to both the velocity and its Laplacian $\nabla^2\underline{u}$. The acceleration is obtained from the velocity time series by a second-order finite difference, and the pressure

gradient following the fluid particle is then recovered by using Eq. 1. In the simulations the turbulence is forced (to achieve stationarity), but since forcing is applied to the large scales only, its direct contribution to the acceleration is small.

PRESSURE GRADIENT, VORTICITY AND STRAIN RATE

The magnitude of the pressure gradient vector is expected to be at least as intermittent as its coordinate components. Instead of attempting to parameterize the functional form of the tails of its PDF, here we consider whether $|\nabla p|$, as a non-negative variable, can be regarded as approximately log-normal. Figure 1 shows the PDF of $\ln|\nabla p|$ at different grid resolutions (and Reynolds numbers). A Gaussian core is clearly evident. At the Reynolds number increases the variance of $\ln|\nabla p|$ increases (showing greater intermittency) while some definite deviation from log-normality (see moments in Table 1) persists.

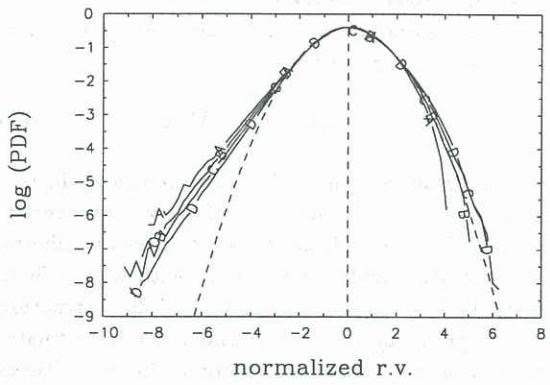

Figure 1: Standardized PDFs of $\ln|\nabla p|$ at grid resolutions 64^3, 128^3, 256^3 and 512^3 (lines A to D). Base-10 logarithms are taken and compared to a Gaussian (dashed curve).

Table 1: Moments of $\ln|\nabla p|$ at different grid resolutions and Taylor-scale Reynolds numbers (R_λ). The symbols σ^2, μ_3 and μ_4 denote variance, skewness and flatness respectively.

Grid	64^3	128^3	256^3	512^3
R_λ	38	96	140	233
σ^2	0.442	0.517	0.574	0.641
μ_3	-0.233	-0.107	-0.002	0.063
μ_4	3.451	3.413	3.359	3.352

Figure 2 compares the PDFs of the logarithms of $|\nabla p|$, $|\underline{\omega}|$ and S. Indirectly we are also comparing the squared pressure gradient, enstrophy and dissipation with a log-normal distribution. Together with the moments in Table 2, we observe that S is closest to log-normal, followed by $|\underline{\omega}|$ (which is most intermittent) and $|\nabla p|$. In classical intermittency arguments log-normality is associated with non-negative variables which represent the small scales. The deviations seen for $|\nabla p|$ are consistent with pressure gradients in fact having strong intermediate-scale content.

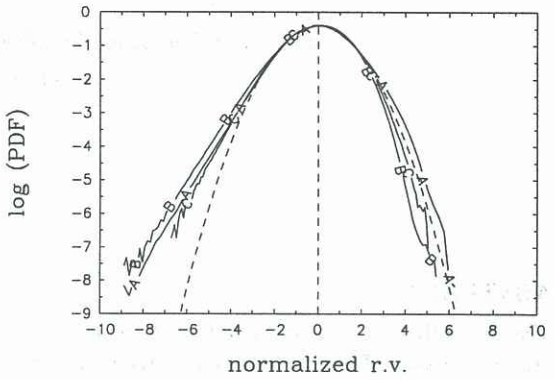

Figure 2: Standardized PDFs of logarithms of $|\nabla p|$, $|\underline{\omega}|$ and S at 512^3 resolutions. The scaling used is similar to Figure 1.

Table 2: Moments of $\ln|\nabla p|$, $\ln|\omega^2|$ and $\ln|S^2|$ from 512^3 simulations.

	$\ln\lvert\nabla p\rvert$	$\ln\lvert\omega^2\rvert$	$\ln\lvert S^2\rvert$
σ^2	0.641	2.470	1.262
μ_3	0.063	-0.319	-0.114
μ_4	3.352	3.279	3.072

To explore the statistical relationships between $|\nabla p|$ and other variables first show the joint PDFs of $|\nabla p|$ and $|\underline{\omega}|$, and of $|\nabla p|$ and S, in Figures 3 and 4. Contour levels in octaves (as opposed to linear intervals) are chosen in order to provide more information on lower-probability regions of the sample space, although adequate representation of the low-probability events that characterize intermittency is still difficult. The relative smoothness of the contours shown indicates good sampling quality achieved from having 512^3 samples in one realization compared to grids at lower resolution. The two sets of contours are similar in shape above the diagonal, but not below. At higher values of the normalized variables the approximate symmetry of the $(|\nabla p|, |\underline{\omega}|)$ contours suggests a strong association between high pressure gradients and high vorticity. The $(|\nabla p|, S)$ contours show a bulge towards high pressure gradients, which indicate that high $|\nabla p|$ and low S is a more likely combination than low $|\nabla p|$ and high S.

Questions like how strongly is high pressure gradient associated with high vorticity are answered more effectively in terms of conditional PDFs. Figure 5 shows that conditional PDFs of $|\nabla p|$ given $|\underline{\omega}|$ and S

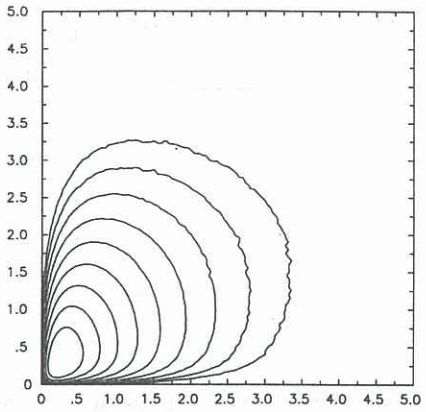

Figure 3: Contours of joint PDF of $|\nabla p|$ (x-axis) and $|\underline{\omega}|$ (y-axis) from 512^3 simulation. Each variable is normalized by its r.m.s value.

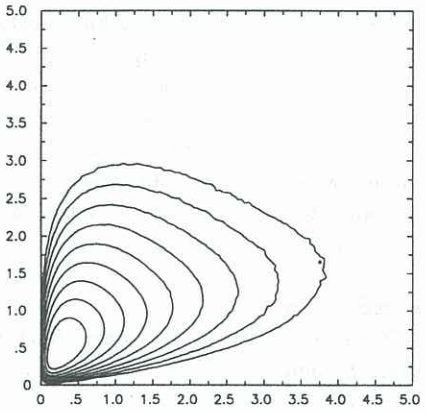

Figure 4: Same as Figure 3, for $|\nabla p|$ and S.

are remarkably similar, and both indicate that pressure gradient is likely to be low in regions of weak local deformation (for both vorticity and strain). For higher vorticity or strain the conditional PDF of $|\nabla p|$ is more spread out, with moderate values of $|\nabla p|$ being most likely but also an appreciable incidence of high pressure gradients.

Differences between vorticity and strain rate are apparent in the their PDFs of $|\underline{\omega}|$ and S conditioned on $|\nabla p|$ in Figure 6. For low $|\nabla p|$ both $|\underline{\omega}|$ and S tend to be low, especially for $|\underline{\omega}|$. For high $|\nabla p|$ the differences are more pronounced: although these conditional PDFs peak at moderate $|\underline{\omega}|$ and S the likelihood of large values of $|\underline{\omega}|$ is substantially greater. Physically this suggests that fast-accelerating fluid particles are more likely to be found in regions of high vorticity than regions of high strain rate.

The observation above has some interesting consequences for the turbulent dispersion of fluid particle pairs, where it may be noted that local straining causes the particles to move apart, but local rotation

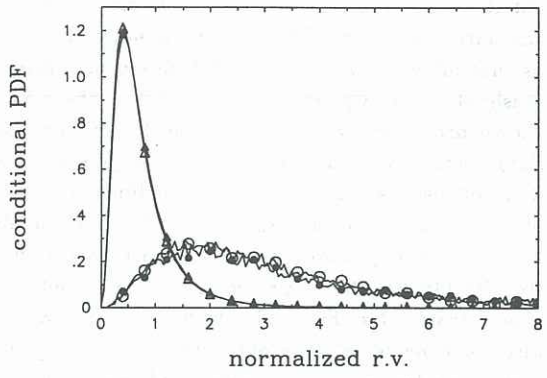

Figure 5: PDF of $|\nabla p|$ given $|\underline{\omega}|$ (open symbols) and S (closed symbols) Triangles and circles for conditioning at 1 and 4 r.m.s respectively.

merely causes them to change their direction of motion relative to each other. In this context, the data suggest that intense strain rate which causes particle pairs to burst away from each other is a rather sporadic event. However, because only one-point PDFs are shown here, a direct connection can be claimed only for particle pairs which are instantaneously close to each other on the Kolmogorov scale.

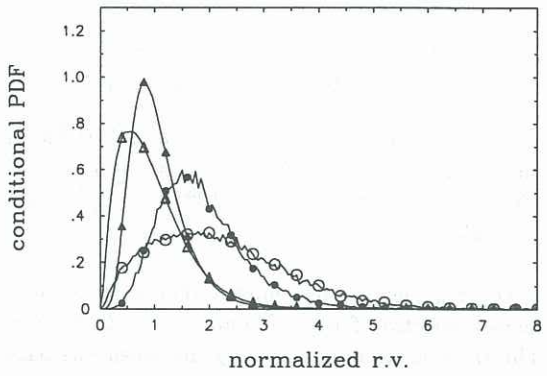

Figure 6: PDFs of $|\underline{\omega}|$ and S given $|\nabla p|$. Symbols same as in Figure 5.

PRESSURE GRADIENT AND LAGRANGIAN ACCELERATION

In the Lagrangian framework one is interested in how quickly a flow variable changes with respect to an observer moving with the flow, or for how long a "memory" of the past is retained. This information is in part expressed by the Lagrangian autocorrelation function, which is the correlation coefficient between the variable fluctuation at two instant of time (say t and $t+\tau$). For stationary turbulence this is a function of time lag (τ) only.

In Figure 7 we compare the autocorrelations of the pressure gradient and viscous acceleration (averaged over the three coordinate components) at two differ-

ent Reynolds numbers, Because of its large variance, the autocorrelation of ∇p is the virtually the same as that of the acceleration (which would be indistinguishable from ∇p on the plot). All of the curves shown drop steeply at small τ, which suggests that fluid particles remain in regions of large pressure gradient or viscous acceleration only for limited periods of time. The results for ∇p are similar to those obtained using a "passive-vector" approach by Gotoh & Rogallo (1994) who neglected the viscous contributions. Just as for the acceleration (which has a zero integral time scale), the autocorrelation of ∇p has a negative trough that becomes shallower at higher Reynolds number. For $\nu\nabla^2\underline{u}$ one may expect some degree of small-scale universality: its integral time scale is found to be about 1.7 τ_η, possibly decreasing slightly with Reynolds number.

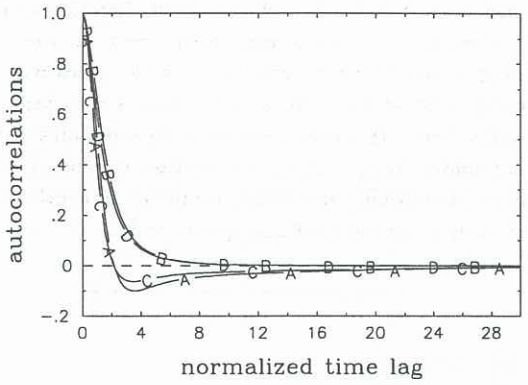

Figure 7: Autocorrelations of ∇p and $\nu\nabla^2\underline{u}$ (circles) versus time lag (τ/τ_η). Lines A, B (∇p, $\nu\nabla^2\underline{u}$) for data at R_λ 230 (512^3) and C, D for R_λ 140 (256^3).

For frequency content information we show the frequency spectra of both ∇p and $\nu\nabla^2\underline{u}$ in Figure 8. The spectra are normalized by the mean dissipation rate ($\langle\epsilon\rangle$) for comparison with classical inertial range scaling for the acceleration spectrum, namely

$$A^L(\omega) = B_0\langle\epsilon\rangle \qquad (2)$$

where B_0 is an universal constant at sufficiently high Reynolds number. A plateau is indeed obtained in an intermediate frequency range where the spectrum of ∇p dominates that of $\nu\nabla^2\underline{u}$ by more than 1.5 orders of magnitude, such that the DNS data suggests a value of about 2.0 for B_0. At higher frequencies these spectra appear to follow respective power laws of exponent about -5 and -3 but numerical noise makes the data for ∇p less reliable in the range $\omega \gg \omega_\eta$.

CONCLUSION

In summary, we emphasize the value of complementary descriptions of pressure gradient statistics from both Eulerian and Lagrangian viewpoints. Consideration of joint and conditional PDFs based on high-resolution direct numerical simulations suggest that fluid particles experiencing large acceleration are more likely to be in regions of high vorticity than those of high strain rate. This has implications for the influence of flow structure on turbulent dispersion. Lagrangian statistics of the pressure gradient and viscous acceleration are also computed separately to give more detailed understanding.

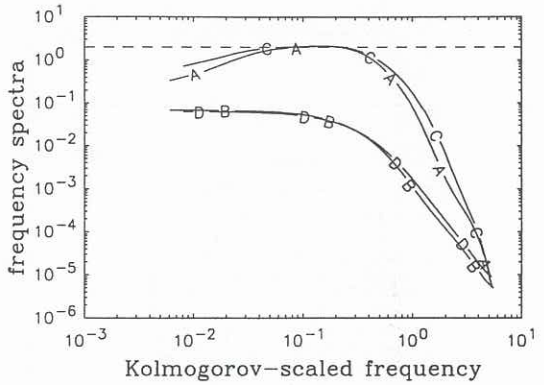

Figure 8: Lagrangian frequency spectra corresponding to the data in Figure 7, normalized by $\langle\epsilon\rangle$, versus frequency (ω) scaled by $\omega_\eta = \pi/\tau_\eta$.

This work was supported in part by The National Science Foundation in the USA.

REFERENCES

BATCHELOR, G.K., "Pressure fluctuations in isotropic turbulence", *Proc. Camb. Phil. Soc.*, **47**, 359-374, 1951.

HILL, R.J. and WILCZAK, J.M., "Pressure structure functions and spectra for locally isotropic turbulence", *J. Fluid Mech.*, **296**, 247-269, 1995.

NELKIN, M. and CHEN, S., "The scaling of pressure in isotropic turbulence", *Phys. Fluids*, **10**, 2119-2121, 1998.

PUMIR, A., "A numerical study of pressure fluctuations in three-dimensional, incompressible, homogeneous, isotropic turbulence", *Phys. Fluids*, **6**, 2071-2083, 1994.

VEDULA, P. and YEUNG, P.K., "Similarity scaling of acceleration and pressure statistics in numerical simulations of isotropic turbulence", Submitted to *Phys. Fluids*, 1998.

VOTH, G.A., SATYANARAYAN, K. and BODENSCHATZ, E., "Lagrangian acceleration measurements at large Reynolds numbers", *Phys. Fluids*, **10**, 2268-2280, 1998.

YEUNG, P.K., "One- and two-particle Lagrangian acceleration correlations in numerically simulated homogeneous turbulence", *Phys. Fluids*, **9**, 2981-2990, 1997.

YEUNG, P.K. and POPE, S.B., "Lagrangian statistics from direct numerical simulations of turbulence", *J. Fluid Mech.*, **207**, 531-586, 1989.